

Noise Reduction of a Model-Scale Landing Gear Measured in the Virginia Tech Aeroacoustic Wind Tunnel

Marcel C. Remillieux,¹ Hugo E. Camargo,² Patricio A. Ravetta,³ Ricardo A. Burdisso,⁴ and Wing F. Ng.⁵
Virginia Polytechnic Institute and State University, Blacksburg, VA, 24061

The effectiveness of various fairings for landing gear noise reduction was measured in the Virginia Tech (VT) Stability Wind Tunnel. This wind tunnel was recently upgraded to an aeroacoustic facility, which allowed acoustic measurements to be carried out in the far-field, out of the flow, and in a low reverberant environment. The model was a very faithful replica of the full-scale landing gear, designed to address the issues associated with low-fidelity models. A 63-element microphone phased array was used to locate the noise source components of the landing gear in its baseline and streamlined configurations, and to measure the noise reduction potential of the fairings. Measurements were carried out from two far-field positions on the flyover path of the landing gear. Through a comparison between the noise levels of the landing gear with and without fairing, the noise reduction potential of each fairing could be estimated. The results from these experiments also showed that if phased-array measurements of the landing gear noise are carried out in the near-field, the noise reduction potential of the fairings could be largely overestimated.

I. Introduction

THE expected growth in air traffic is likely to increase the noise impact on the communities surrounding airports as well as the need for further airframe noise reduction. With the introduction of high-bypass ratio turbofan engines in the 1970s, significant engine noise reduction could be achieved. At take-off, maximum engine power is required and engine still constitutes the principal noise source. However, on approach to landing, aircraft operate at lower thrust and airframe noise has become comparable to engine noise. In the case of some modern aircraft, airframe has even become the predominant noise source in the landing phase.

It was shown that high lift devices (flaps and slats) and landing gears are the dominant airframe noise components.¹ Airframe noise was also shown to be highly dependent on the aircraft size. For instance, in the case of large capacity aircraft, airframe noise is dominated by landing gears.²

Within the European research program RAIN, some noise reduction concepts were tested on full-scale Airbus A340 main and nose landing gears, in an open-jet wind tunnel.³ A noise reduction of up to 3 dB on the forward-arc was achieved with a combination of fairings streamlining the major landing gear noise components. Major aircraft noise reduction programs have also been launched in the United States since the early 1990s. In 2005, Boeing, associated with General Electric Aircraft Engines, Goodrich Corporation, NASA, and All Nippon Airways, conducted a three-week flight test program on a Boeing 777, under the name QTD2 (Quiet Technology Demonstrator). More details about the program are given in reference 4. During these tests, a fairing designed by Goodrich was mounted on the 777's main landing gear to streamline the truck. The landing gear truck fairing used in the flight tests was based on the measurements and evaluation of multiple fairing designs tested on a high-fidelity, small-scale gear model, in a hard-walled wind-tunnel.⁵ In other words, measurements were carried out in the near-field and in a highly reverberant environment. In addition to the truck fairings provided by NASA, various fairings were developed at Virginia Tech (VT). Microphone phased-arrays allow for noise sources to be located almost regardless of the background noise levels. However, it was shown by the authors⁶ that near-field phased-array measurements of the landing gear noise on the flyover path are not truly representative. When the array is in the

¹ Graduate Research Assistant, Mechanical Engineering Department, MC 0238, Student Member AIAA.

² Graduate Research Assistant, Mechanical Engineering Department, MC 0238, Student Member AIAA.

³ Ph.D. Alumnus, Mechanical Engineering Department, MC 0238, Member AIAA.

⁴ Professor, Mechanical Engineering Department, MC 0238, Member AIAA.

⁵ Chris Kraft Endowed Professor, Mechanical Engineering Department, MC 0238, Associate Fellow AIAA.

near-field, straight under the gear, the truck acts like an acoustic shield and the landing gear components located behind the truck such as the strut, braces, and lock links are hidden from the array. The authors⁶ also showed that in the far-field, taking acoustic measurements straight under the model only is not sufficient to characterize landing gear noise on the flyover path.

To address these issues and measure as accurately as possible the noise reduction potential of the fairings previously tested in a hard-walled wind tunnel,^{5,7} tests were repeated in the VT aeroacoustic wind tunnel. Phased-array measurements of the landing gear noise with and without fairing were carried out from two far-field positions, straight under the gear and on the rear-arc of the gear.

This paper is organized as follows. Section 2 describes the experimental setup, which includes the model scale landing gear, the streamlining devices, the microphone phased-array and data post-processing, the wind tunnel facility, and the testing configurations. Section 3 reports the experimental results. First, noise reduction of the truck and of the strut and braces is discussed qualitatively with the beamforming maps of the landing gear noise with and without fairings. Subsequently, noise reduction is quantified by integration of the beamforming maps. Conclusions are given in Section 4.

II. Experimental Setup

A. Landing Gear Model

Experiments were conducted on a high-fidelity, 26%-scale model of the Boeing 777 main landing gear. This model, provided by NASA, was designed to address the issues associated with low fidelity models. Figure 1 shows the Boeing 777 landing gear model. The key gear components are also identified in this figure. The major parts constituting the primary structural framework were made of steel and aluminum. Using stereo lithography, most of the full-scale details were reproduced with accuracy down to 0.12 inch in full scale. The details include wheel hubs, brakes cylinders, hydraulic valves, and so forth. Other significant details, not present in the low-fidelity model, are the hydraulic lines and cables that were reproduced using electrical wires. Although the small-scale model is a very faithful representation of the full-scale gear, several details were omitted. For instance, the small door mounted on the top of the main door in the full-scale landing gear, is not present in the 26%-scale model. Also, wheel hubs in the model do not allow air to pass through. Finally, the wing cavity, where the landing gear is stored in the cruise configuration of the aircraft, is not modeled.

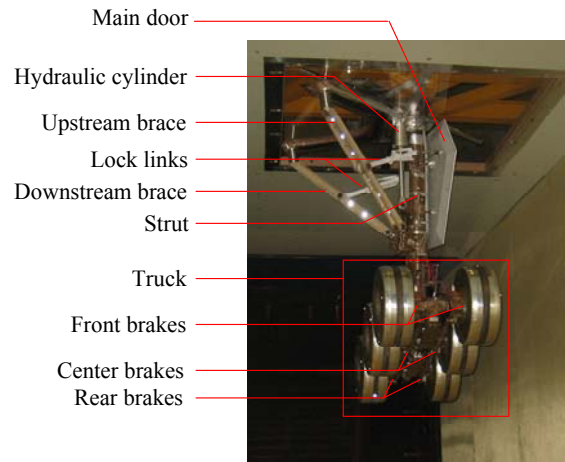


Figure 1: The 26%-scale, high-fidelity, Boeing

B. Streamlining Devices

Three fairings were developed at Virginia Tech by Ravetta⁸ to streamline the landing gear components identified as major noise sources. Figure 2a is a photograph of the landing gear as fitted with the VT-lower-truck, -strut, and -braces fairings. The devices were made of a double-layer of elastic “lycra-like” cloth and were held in place with Velcro. The material used was light, stretchable, strong, and did not interfere with the steering mechanism of the landing gear. The devices streamlined the truck, the braces, and the strut. A more comprehensive description of the fairings design may be found in reference 8. A rigid fairing streamlining the lower truck and referred to as NASA toboggan was also tested. Figure 2b depicts the landing gear as fitted with the NASA toboggan. Originally, this fairing was designed by NASA, the Boeing Co., and Goodrich, for mitigation purposes in the QTD2 Program.

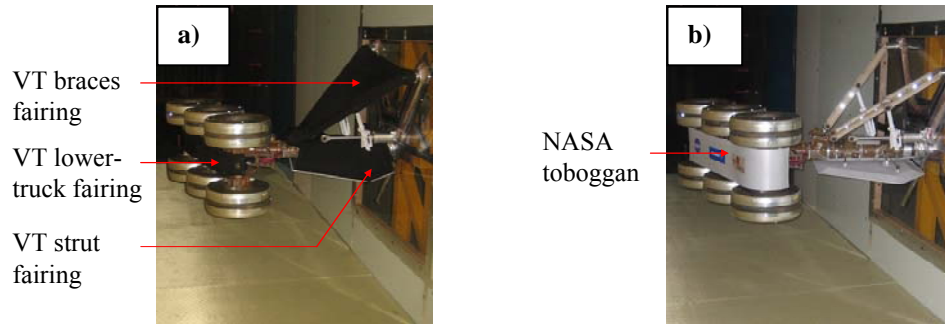


Figure 2: Photographs of a) the VT fairings and b) the NASA toboggan mounted on the landing gear.

C. Wind Tunnel Facility

The landing gear was installed in the VT Stability Wind Tunnel. Originally it was a NACA facility located at Langley Field in Virginia, designed to provide a very low turbulence-level flow for dynamic stability measurements. Figure 3 is a schematic description of the VT Stability Wind Tunnel in its original hard-walled configuration. The facility is a continuous, single return, subsonic wind tunnel. The tunnel is powered by a 0.45 MW variable speed DC motor driving a 14.1 ft. propeller at up to 600 rpm. Although the tunnel forms a closed loop, it has an air-exchange tower open to the atmosphere to allow for temperature stabilization. The air exchange tower is located downstream of the fan and motor assemblies. Downstream of the tower, the flow is directed into an 18 x 18 ft. settling chamber containing 7 turbulence-reducing screens, each with an open area ratio of 0.6 and separated by 5.9 inches. The test section is 24 ft. long with a constant square cross section of 6 ft. The flow passing through the test section undergoes a 9:1 area contraction. The test section is enclosed in an air-tight control room so that the pressure in the control room equates the pressure in the test section via a window located downstream of the test section. The problem of air leakage into the test-section flow is thus minimized. At the downstream end of the test section, flow passes into a 3-degree diffuser. The four corners in the flow path (two between the air exchange tower and settling chamber, and two between the diffuser and fan) are equipped with diagonal arrays of shaped turning vanes.

Since its installation at Virginia Tech, the wind tunnel has undergone a series of modifications such as the renovation of the fan and the re-insulation of the motor windings, resulting in the increase of the overall tunnel efficiency. Although the Stability Wind Tunnel was shown to have very good flow quality and was used for aeroacoustic measurements in the past, it was not primarily built as a quiet facility.

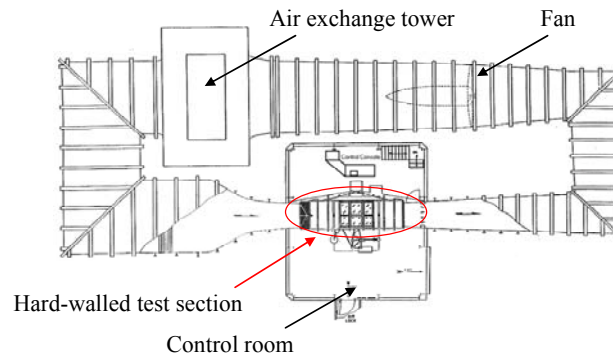


Figure 3: Schematic of the VT Stability Wind Tunnel in its original hard-walled configuration.

Recently, as a part of a project to render the Stability Wind Tunnel suitable for aeroacoustic measurements, the hard-walled test section was removed and replaced by an anechoic system. Figure 4a is a CAD drawing of the test section in its semi-anechoic configuration. Note that the test section may also be used in a fully-anechoic configuration. The semi-anechoic configuration was necessary in this case in order to mount the landing gear sideways in the test section. The bottom and the top of the test section (Figures 4a and b) were fitted with acoustic treatment. Stretched Kevlar® membranes glued on perforated metal sheets separated the flow area from the acoustic treatment. A hard wall with a window was mounted on one side to allow for the model to be mounted sideways in the

test section. An anechoic chamber (Figure 4c) was mounted on the side opposite to the model and the corresponding hard-wall was replaced by a Kevlar window (Figures 4b and c). Due to the presence of the landing gear in the test section, the center of the Kevlar window was deflected toward the anechoic chamber, which potentially produced a change in local flow speed around the landing gear. However, the amplitude of the deflection was relatively small, e.g. estimated to be less than an inch at $M = 0.17$. Such deflection caused a change in flow speed of about 1%, which is insignificant.

Stretched Kevlar® membranes were first utilized in aeroacoustic measurements by Jaeger et al.⁹ as an answer to flow induced noise. Relevant properties of Kevlar for aeroacoustic measurements were shown to be, (i) very high strength and durability that makes it tolerate flow-induced fatigue very well, (ii) when stretched, it appears as a hard surface to the flow, and (iii) very low acoustic impedance up to high frequencies. Depending on the type of fabrics utilized, the acoustic attenuation may vary. In this application, 120 style, 1.7 oz/in², plain weave Kevlar was chosen. Jaeger et al.⁹ found that the insertion loss varied from nearly 0 at low frequencies to about 2 dB at 25 kHz.

While the flow was contained in the test section, the sound generated by the model was allowed to propagate through the Kevlar to the anechoic chamber where the phased array was located. In this sense, this hybrid facility is similar to an open-jet wind tunnel from an acoustic point of view and to a hard-walled wind tunnel from a fluid point of view.

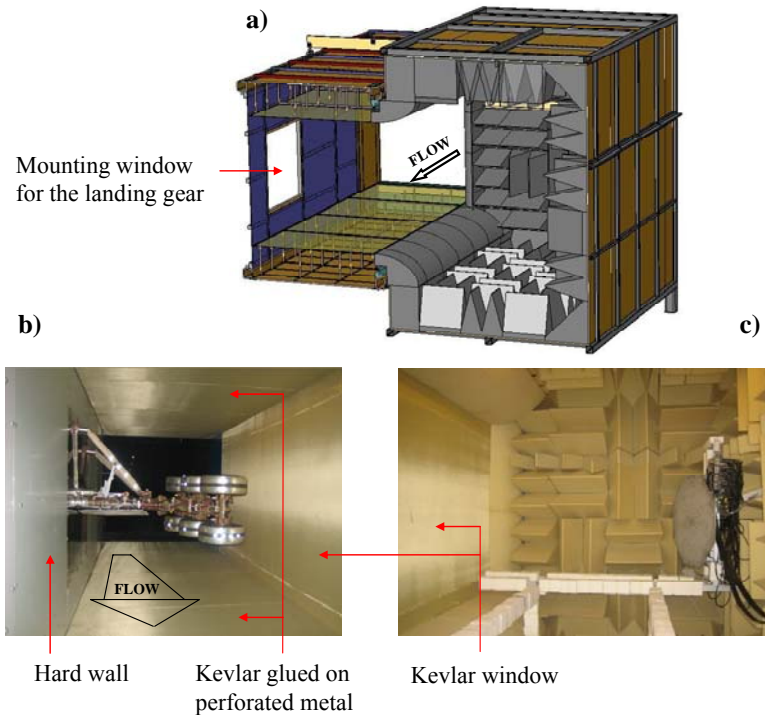


Figure 4: a) A 3D-CAD drawing of the semi-anechoic test section, b) the 26% scale landing gear mounted in the test section, and c) the 63-element microphone phased array installed in the anechoic chamber.

D. Microphone Phased-Array and Post-Processing

The acoustic data acquisition was carried out with the 63-element microphone phased array depicted in Figure 5a. This array was designed for VT by J. Underbrink and R. Stoker from the Boeing Co. The microphones of the phased array (Panasonic WM-60AY Electret microphones) were patterned in a multi-arm spiral manner as depicted in Figure 5b. The microphones were found to be reliable only up to about 20 kHz, i.e. the microphone signal rolled off steeply around 20 kHz. An aluminum plate was used to position the microphones accurately. Tapped holes in the plate, at the microphone locations, allowed the custom-made microphone adaptors to be bolted in the plate so that the microphones were mounted flush with the plate surface.

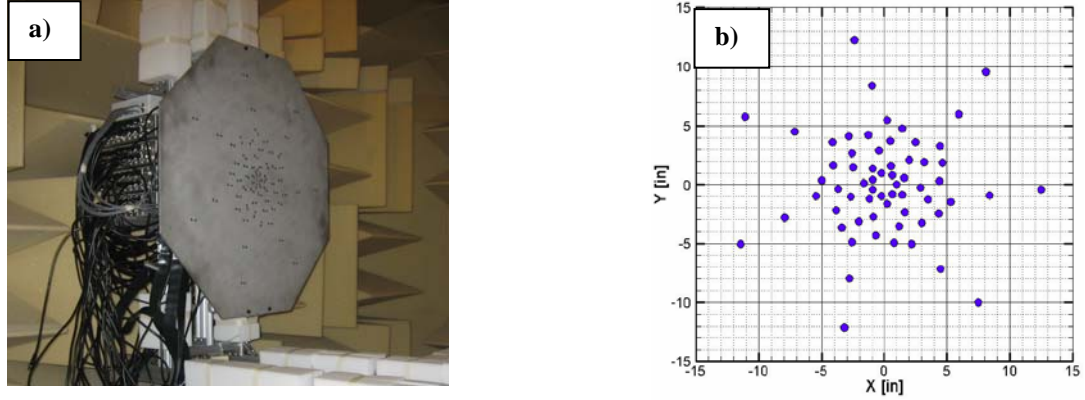


Figure 5: a) The 63-element microphone phased array and b) the microphone pattern of the array.⁸

The 63 microphones signals were sampled simultaneously at 51200 samples per second in 25 separate blocks of 16384 samples each. Time domain data were processed using a frequency-domain, phased array beamforming code developed at VT that accounts for the flow in the test section and the sound refraction through the flow velocity discontinuity between the test section and the anechoic chamber. As shown in Figure 6, when sound propagates from source points to a microphone of the array, part of the acoustic path is in the flow and part is outside of it. If conventional beamforming is used, an apparent source will be located downstream of the actual source. In the revised beamforming algorithm used here, the components of the steering vector were given by the solution of the convected wave equation,

$$C_j(\bar{x}_n) = \frac{e^{-ikr_j}}{4\pi R_j} \quad (1)$$

where \bar{x}_n are the coordinates of the grid point where the array is being steered to, k is the wave number, R_j is the distance between the grid point with coordinates \bar{x}_n and the microphone j , and r_j is the distance traveled by the ray to the microphone j . The ray path is computed by following the numerical ray tracing technique developed by Candel¹⁰ and summarized by Pierce.¹¹

Acoustic data were processed from 2 to 20 kHz in 1/12th octave bands. The spatial resolution of the array will be given in terms of the beamwidth (BW), i.e. the region of the beamforming map within 3 dB of the peak level. Thus, for a plane located at 117 inches from the array, the beamwidth was found to be $BW_{117} = 7.53 \lambda$, where λ is the sound wavelength. The signal to noise ratio (SNR) as a function of frequency, for a vertical plane at 117 inches from the array, is given in Figure 7. The lowest SNR is about 9.8 dB at 20 kHz.

In all cases, the post-processing was carried out over the same scanning grid. Such scanning grid, with dimensions 70 x 56 x 39 inches, contained 323031 points and encompassed the entire landing gear.

The array was calibrated for phase to account for phase mismatch in the microphone signals and for errors in microphone positions. The array was also calibrated for amplitude. Tests were conducted in the VT semi-anechoic wind tunnel to determine the sensitivity of the array, to account for the presence of the Kevlar window, and the dissipation effects due to the flow.

Note that the array of microphones was mounted on a finite plate. For this reason, the signals recorded by the microphones located close to the edge of this plate may be subjected to edge effects, e.g. diffraction, scattering. For the calibration of the phased-array, a monopole-like source was installed at various locations in the test section and its noise levels were measured both with a single microphone and the phased-array. Levels obtained with the single microphone and the integrated spectra are virtually the same.¹² Therefore, edge effects on the results are likely to be small and were not accounted for in this study.

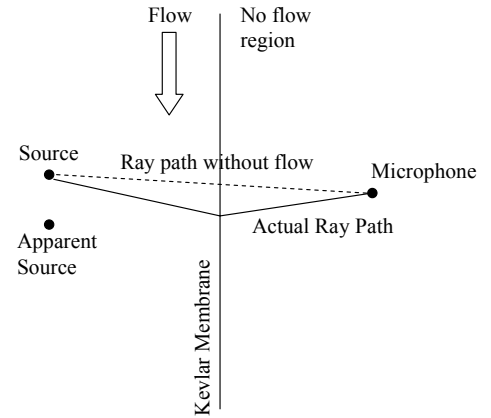


Figure 6: Sound wave propagation through a flow velocity discontinuity using ray acoustics

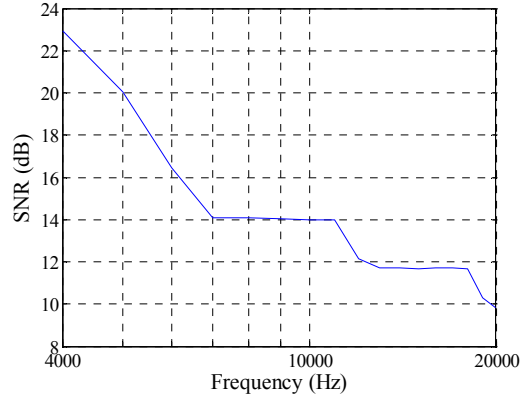


Figure 7: Signal to noise ratio of the array as a function of frequency for a vertical plane at 117 inches from the array.

E. Testing Configurations

Figure 8 is a schematic description of the experimental setup. The microphone phased-array was positioned in such a way as to take acoustic data on the flyover path of the model, i.e. the center of the array was at the mid-height of the test section. The array in position labeled 1 was located straight under the landing gear, 82.5 inches from the Kevlar wall. The distance d between the array and the model was sufficiently large for the array to be in the acoustic far field ($d > 10\lambda$) and nearly in the geometric far field (d was about 3 times the largest dimension of the landing gear). Additional far-field measurements were carried out with the array in position 2. In this position, the array was on the rear arc of the landing gear. The center of the array was located 82.5 inches from the Kevlar wall. To avoid distortion effects, the phased array was oriented such that its center was pointing toward the center of the hard-wall window.

Four configurations of the landing gear were tested, the baseline (no fairing), the landing gear fitted with the NASA toboggan, with the VT-lower-truck fairing, and with the three VT fairings.

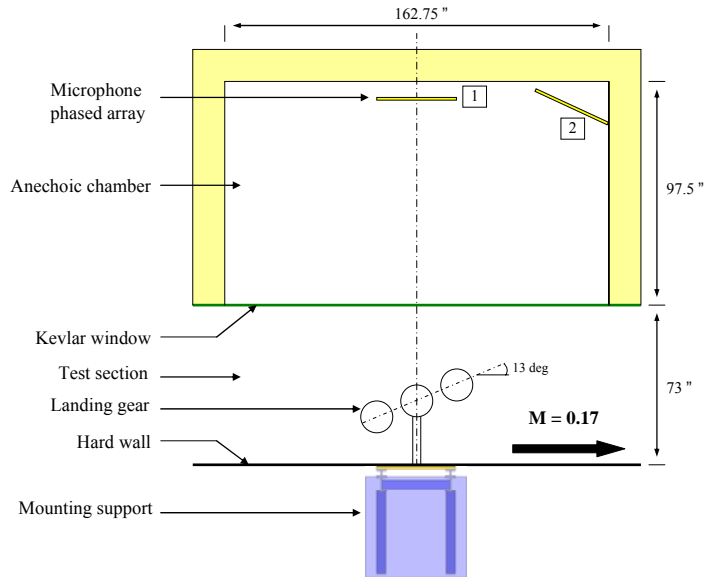


Figure 8: Schematic description (top view) of the test setup for phased-array measurements of the noise reduction potential of the fairings.

III. Results

In this section, the performance of the fairings described in Section II.B is discussed. In past experiments conducted in the hard-walled configuration of the VT wind tunnel, the noise reduction potential of these fairings was measured with the same microphone phased-array but in the near field and in a reverberant environment.^{7,8} It was shown by the authors⁶ that on the near-field flyover path, phased array measurements of the landing gear noise are not truly representative. It was also shown that, in the far-field, noise measurements right under the gear are not sufficient to characterize landing gear noise on the flyover path. Therefore, in the herein study, the noise reduction potential of the fairings is measured from two far-field flyover positions of the phased-array, straight under the gear and on its rear arc.

First, noise reduction is examined qualitatively by comparing the beamforming maps of the landing gear in its baseline configuration and fitted with various fairings. Subsequently, the noise reduction potential of the fairings is quantified by integration of the beamforming maps.

Results are presented for the wind tunnel speed $M = 0.17$, which is close to the maximum achievable speed in the facility. All the frequencies discussed in this section have been scaled to full-scale frequencies using the following relation,

$$f_{full-scale} = scale\ factor * f_{measured} \quad (2)$$

where the scale factor is 0.26.

Phased-array data were post-processed for over 50 frequency bands in $1/12^{th}$ octave bands. It would be very difficult to show beamforming maps at all frequencies. Instead, beamforming maps are shown at selected frequencies. To better aid in the visualization of the key components of the gear noise, cross-sectional plots of the three-dimensional beamforming maps originally generated are presented. The location of the cross-section is depicted in Figure 9a. Results shown on this cross-section are the most representative of the noise generated by the strut, door, braces, and hydraulic cylinder. For the sake of clarity, this plane is referred as “strut” plane in the rest of the paper. Noise generated sources on the truck also appear in the “strut” plane. Depending on the position of the array relative to the gear, the location of the truck noise source components on the “strut” plane will vary. This is well illustrated by the schematic shown in Figure 9b. In this figure and in the rest of the section, FB-x, RB-x, S-x, D-x, UB-x, and DB-x identify the front brakes, rear brakes, strut, door, and upstream- and downstream-brace noise sources, respectively, where x takes values of 1 and 2, corresponding to the two array positions.

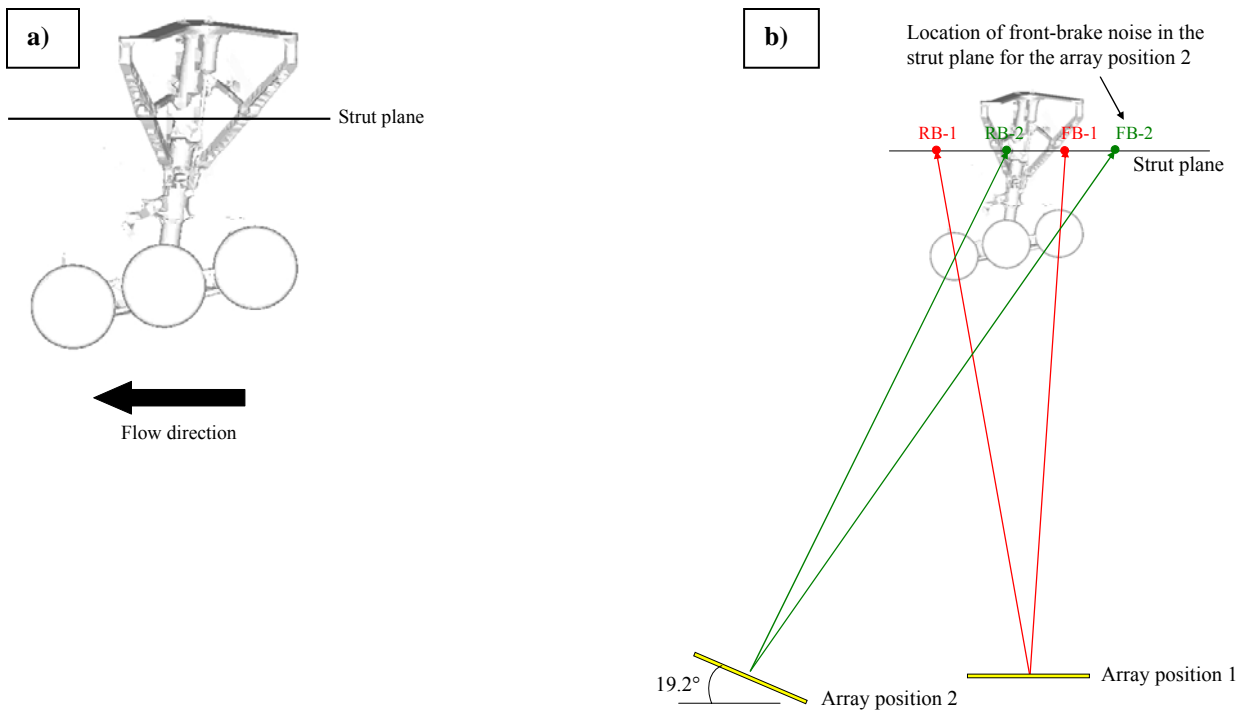


Figure 9: a) Location of the “strut” plane. b) Locations of the front- and rear-brakes noise projected onto the “strut” plane for array positions 1 to 2.

A. Lower-Truck Noise Reduction

Figures 10 and 11 show the beamforming maps of the baseline (top maps), VT-lower-truck-fairing (center maps), and NASA-toboggan (bottom maps) configurations of the landing gear at the full scale frequencies of 3381 and 4782 Hz, respectively.

The beamforming maps of the landing gear fitted with the VT-lower-truck fairing are described first (center maps in Figures 10 and 11). A comparison with the baseline configuration (top maps) indicates that the VT-lower-truck fairing achieves significant noise reduction of the lower truck. For instance, for the array in position 1 (left center maps), the reduction of the peak level in the strut plane due to the VT-lower-truck fairing is about 3.9 and 4.8

dB at 3381 and 4782 Hz, respectively. As noise from the lower truck is reduced, noise from the downstream and upstream braces may be identified more clearly than in the baseline configuration. For the array in position 2 (right center maps), the noise reduction due to the VT-lower-truck fairing is about 2.1 and 1.2 dB at 3381 and 4782 Hz, respectively. For the array in position 2, the truck does not act as an acoustic barrier as it is the case with the array in position 1. In other words, the noise sources behind the truck, for instance the braces and the strut, may now be seen from the array on the rear arc. As a result, the performance of the truck fairing is deteriorated.

Now consider the model fitted with the NASA toboggan. Figures 10 and 11 (bottom maps) indicate that the NASA toboggan is very effective at suppressing noise from the lower truck at 3381 Hz and totally eliminates it at 4782 Hz, i.e. the source cannot be seen by the array. For the array in position 1, at 3381 Hz (Figure 10 – left bottom map), the downstream brace appears as the major noise source. The noise reduction achieved by the NASA toboggan is such that at 4782 Hz (Figure 11 – left bottom map), in addition to the downstream brace, the leading edge of the door may also be identified as a noise source. The door could not be identified in the baseline and VT-lower-truck-fairing configurations (Figure 11 - top and center maps) because landing gear noise was dominated by the truck and braces noise sources. On the rear arc, array in position 2 (Figure 11 – right bottom map), the noise generated by the door cannot be identified, most likely because the truck is no longer an acoustic barrier and the noise levels of the braces have become significantly larger.

Note that for the array in position 2, the strut appears as a major noise source, regardless the type of device streamlining the lower truck. Therefore, the noise reduction potentials of the VT-lower-truck fairing and the NASA toboggan is expected to be poor or not sufficient when viewed from a position other than straight under the landing gear, i.e. the upper landing gear components such as the strut, braces, and so forth are not acoustically shielded by the truck. This implies that an effective noise control of the landing gear must include the strut and braces sources in addition to the truck.

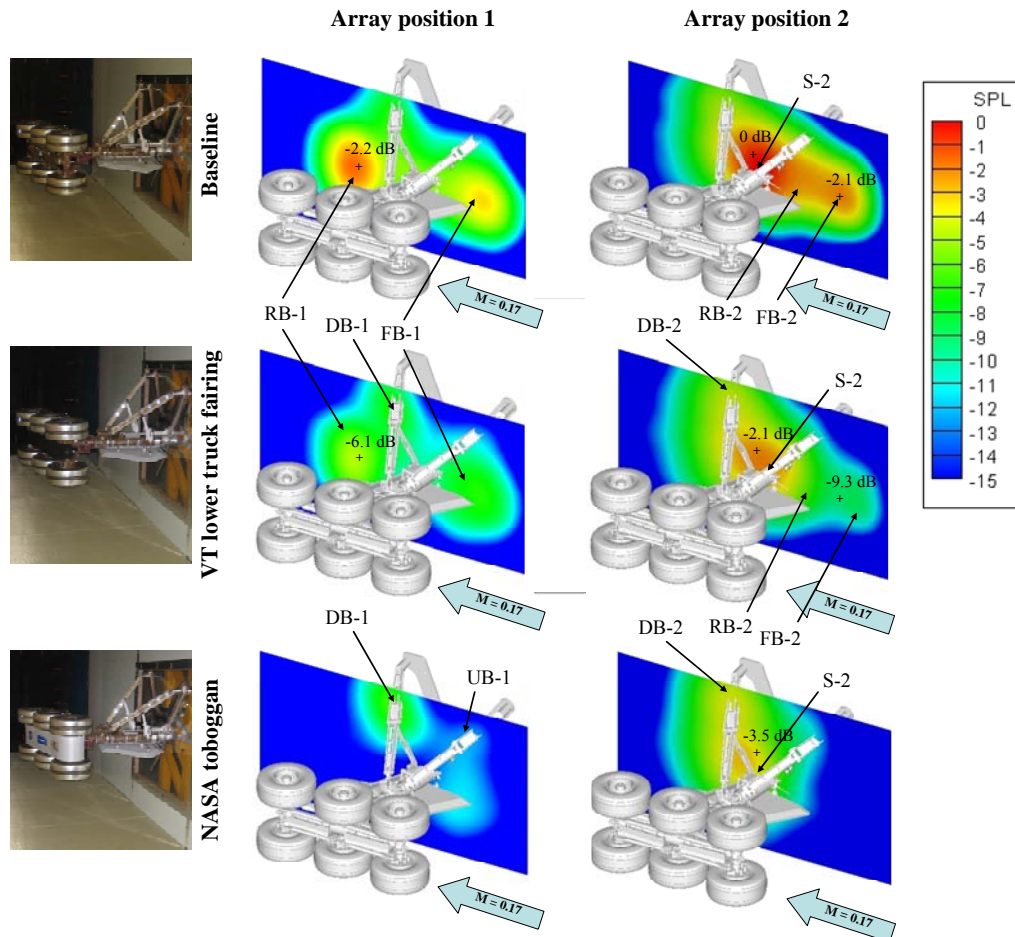


Figure 10: Beamforming maps of the baseline, VT-lower-truck-fairing, and NASA-toboggan configurations of the landing gear at full scale frequency of 3381 Hz, as obtained from array-positions 1 and 2. Peak value of beamforming map of the baseline landing gear with array in position 2 used as reference, i.e. 0 dB.

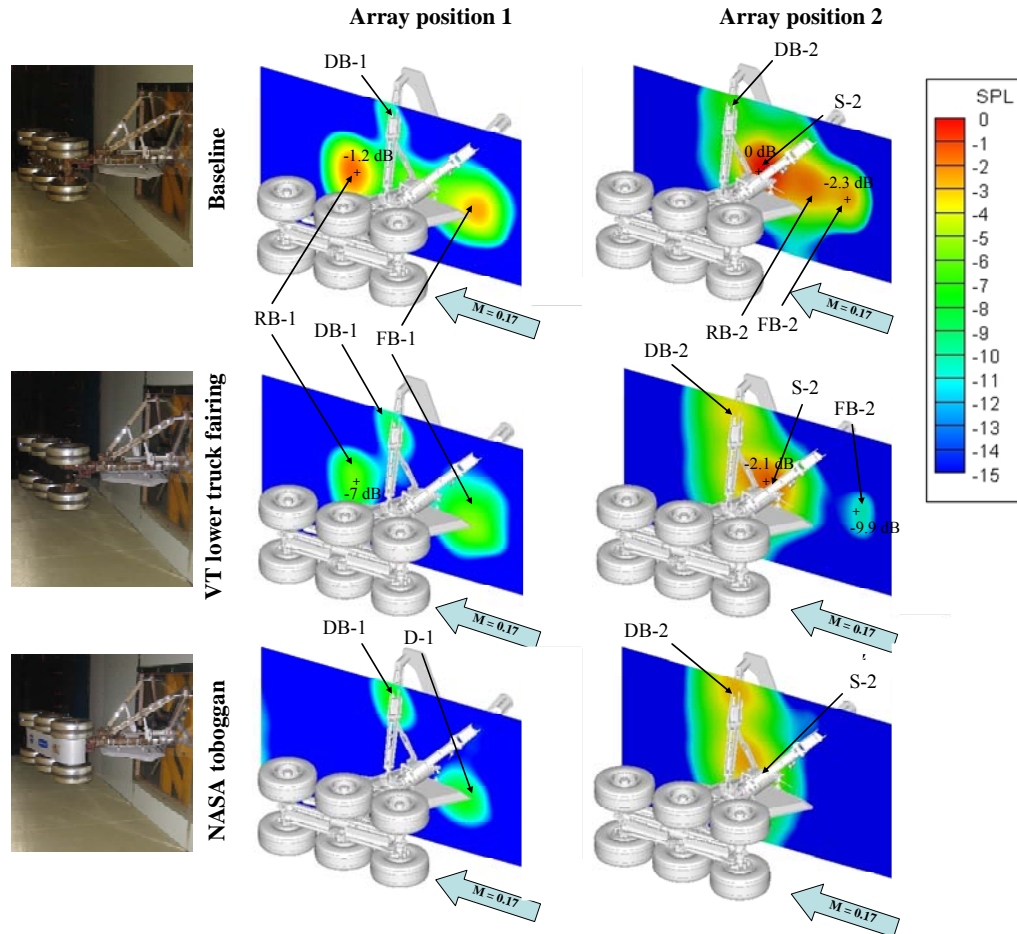


Figure 11: Beamforming maps of the baseline, VT-lower-truck-fairing, and NASA-toboggan configurations of the landing gear at full scale frequency of 4782 Hz, as obtained from array-positions 1 and 2. Peak value of beamforming map of the baseline landing gear with array in position 2 used as reference, i.e. 0 dB.

B. Braces and Strut Noise Reduction

Figures 12 and 13 depict the beamforming maps of the baseline (top maps), VT-lower-truck-fairing (center maps), and all-VT-fairings (bottom maps) configurations of the landing gear. Results are shown for full scale frequencies of 3381 and 4782 Hz in Figures 12 and 13, respectively. The VT-lower-truck-fairing and all-VT-fairings configurations are compared to show the noise reduction achieved by the strut and braces fairings for both far-field positions of the array.

For the array in position 1, noise levels generated by the braces and the door are much lower in the all-VT-fairings configuration than in the VT-lower-truck-fairing configuration. For instance, noise from the downstream brace is reduced by about 6.7 at 3381 Hz and by more than 10 dB at 4782 Hz. For the array in position 2, noise reduction occurs at the links and downstream brace locations. Noise from the downstream brace is reduced by about 5.1 and 2.7 dB at 3381 and 4782 Hz, respectively.

Like the lower-truck-fairings discussed in the previous sub-section, the noise reduction potential of the strut and braces fairings is reduced as the array is moved from straight under the gear (array-position 1) to the rear arc (array-position 2).

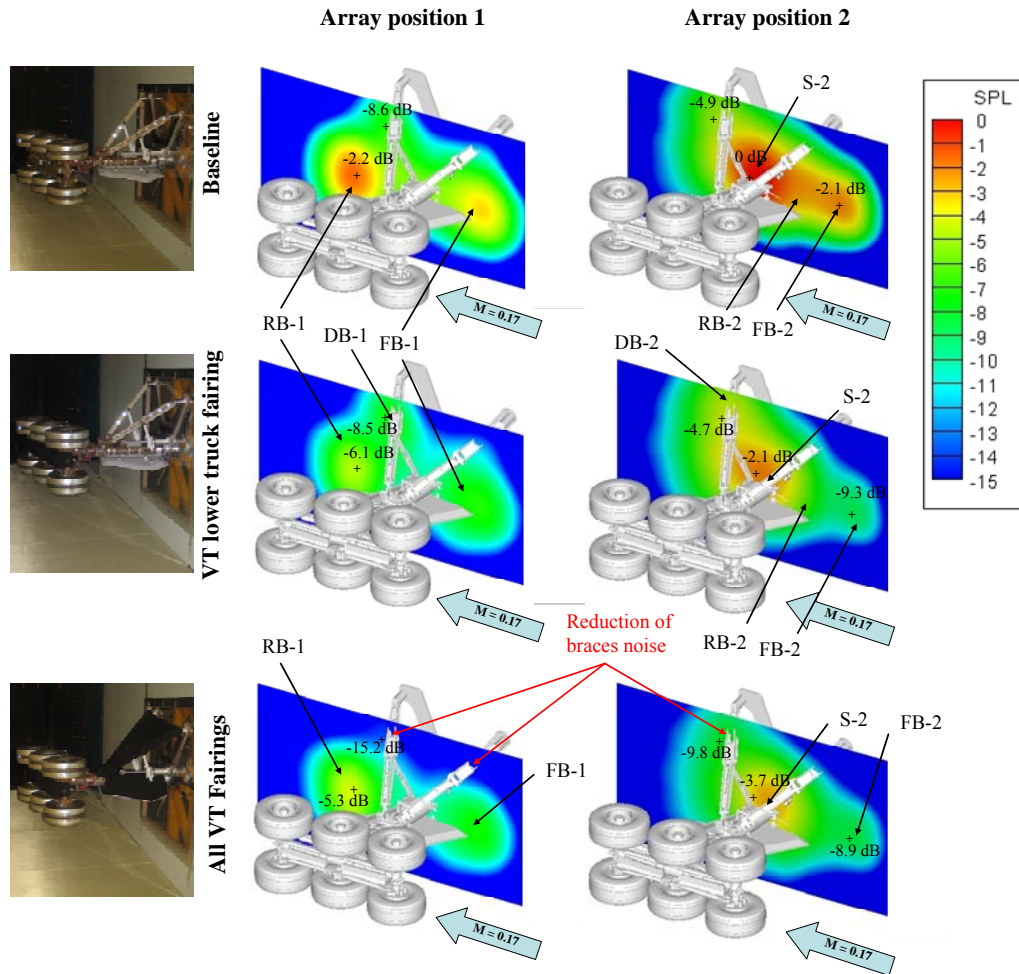


Figure 12: Beamforming maps of the baseline, VT-lower-truck-fairing and all-VT-fairings configurations of the landing gear at full scale frequency of 3381 Hz, as obtained from array-positions 1 and 2. Peak value of beamforming map of the baseline landing gear with array in position 2 used as reference, i.e. 0 dB.

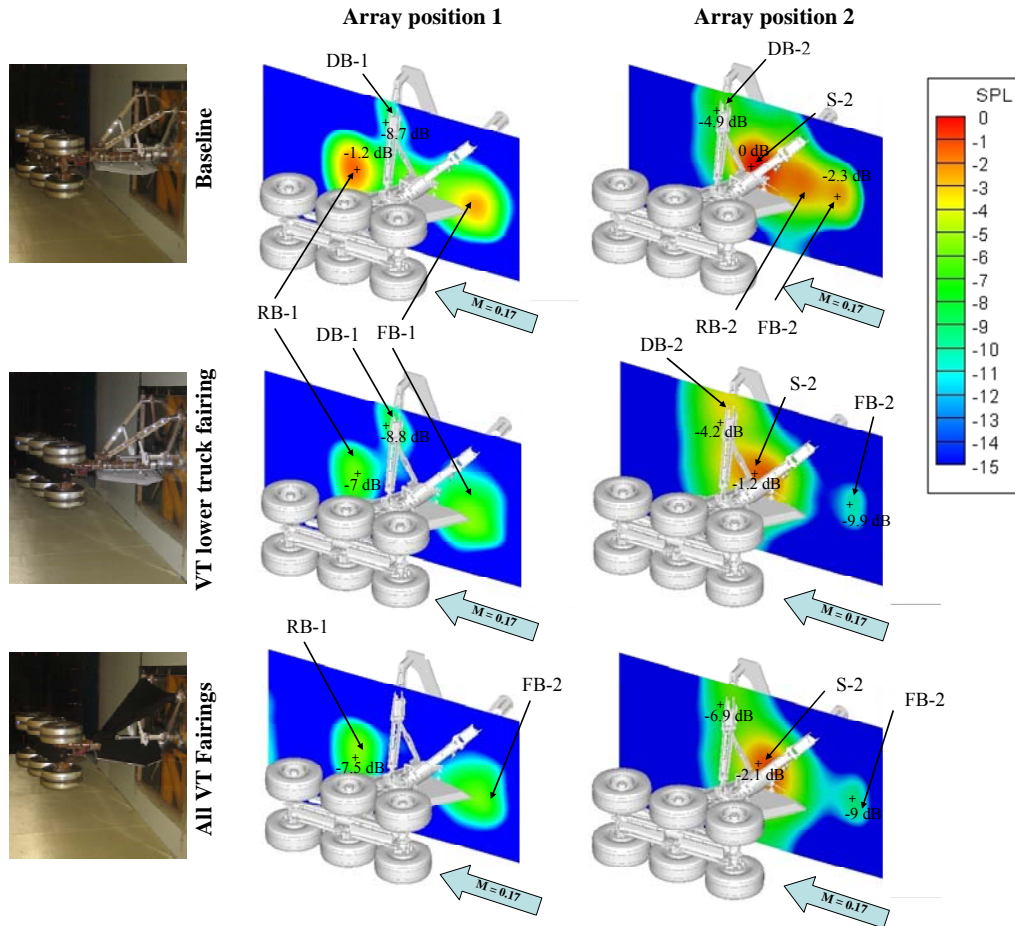


Figure 13: Beamforming maps of the baseline, VT-lower-truck-fairing and all-VT-fairings configurations of the landing gear at full scale frequency of 4782 Hz, as obtained from array-positions 1 and 2. Peak value of beamforming map of the baseline landing gear with array in position 2 used as reference, i.e. 0 dB.

C. Quantification of Landing Gear Noise Reduction

In this section, the noise reduction potential of the fairings is discussed quantitatively by integration of the 3-dimensional beamforming maps encompassing the entire landing gear. The noise reduction is estimated from the spectral difference between baseline and streamlined configurations. Results obtained in hard-walled test section, in the near-field, straight under the gear, are also reported for comparison purposes. No correction has been applied to the data to predict the reduction for an actual flight configuration of the aircraft. These corrections, described in reference 13, are beyond the scope of this study and will not be applied to the results presented in this section.

Figures 14a and b depict the noise reduction due to the NASA toboggan (blue curve), VT-lower-truck fairing (red curve), and all VT fairings (truck, braces, and strut fairings - green curve) as measured with the array in positions 1 and 2, respectively.

Results in Figure 14a indicate that when the array is in position 1, the NASA toboggan achieves up to 7.7 dB noise reduction at 3000 Hz. The VT-lower-truck-fairing and all-VT-fairings configurations have levels up to 3 dB and 4.5 dB lower than the baseline gear, respectively. Therefore, when the array is in position 1, the NASA toboggan is the most effective fairing. This result is consistent with the observations made in Sections III.A and III.B that the NASA toboggan was the most effective truck fairing, producing reductions beyond what the array could identify.

As indicated by the results in Figure 14b, for the array in position 2, the noise-reduction achieved by the NASA toboggan is only up to a maximum of 4 dB at 3000 Hz, as compared to 7.7 dB straight under the gear (array-position 1). As a result, the NASA toboggan and all the VT fairings achieve comparable noise reduction. The effectiveness of the VT-braces and -strut fairings is much more noticeable for the array in position 2 than for the array in position 1. For instance, for the array in position 1 at 5000 Hz, both the VT-truck and all the VT fairings achieved the same 3

dB reduction. On the other hand, for the array in position 2 at 5000 Hz, the all-VT-fairings configuration is 1 dB quieter than the VT-lower-truck-fairing configuration. These observations are in very good agreement with the beamforming maps discussed earlier on. It was shown that, as the array is moved to a position where the strut and the braces are no longer shielded by the lower truck, the effectiveness of a fairing streamlining the lower truck only (VT lower truck fairing or NASA toboggan) is significantly reduced.

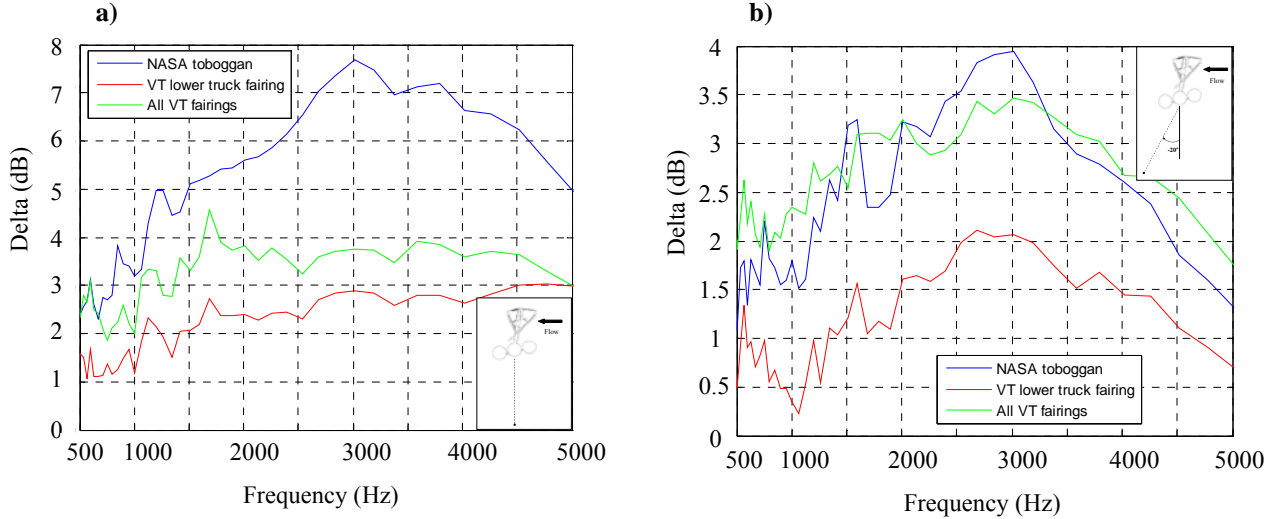


Figure 14: Noise reduction due to the NASA toboggan (blue curve), VT-lower-truck-fairing (red curve), and all VT fairings (truck, braces, and strut fairings - green curve) as estimated with the integrated spectra. The phased array was in the far-field in positions a) 1 and b) 2.

The above results suggest that a larger noise reduction may be achieved if the NASA toboggan is used in conjunction with the VT-braces and -strut fairings. The noise reduction that the braces and strut fairings would achieve alone was estimated. The result was then added to the noise reduction achieved by the NASA toboggan to obtain the noise reduction due to the combination of the NASA toboggan and VT fairings. Let Δ_T , Δ_{SB} , Δ_{TSB} , and Δ_N denote the noise reduction from the VT-lower-truck fairing, VT-strut+braces fairings, VT-truck+strut+braces fairings, and NASA-toboggan, respectively. The noise reduction from the strut+braces fairings may be estimated with the following relation,

$$\Delta_{SB} = \Delta_{TSB} - \Delta_T \quad (3)$$

This estimated noise reduction due to the VT-strut+braces can now be added to Δ_N , the noise reduction due to the NASA-toboggan fairing. Figure 15 depicts the noise reduction due to the NASA toboggan plus the VT-braces and -strut fairings (solid curves) and NASA toboggan alone (dashed curves) as measured with the phased array in the far-field in positions 1 (blue curves) and 2 (red curves). On the flyover path, straight under the landing gear, the noise reduction due to the NASA+VT fairings (solid blue curve) ranges from 3.5 dB at 500 Hz to 8.5 dB at 3000 Hz. On the rear arc (solid red curve), the reduction is more modest and ranges from 2.5 dB at 5000 Hz up to 5.3 dB at 3000 Hz. For both array positions, levels of the solid curve are higher than the ones of the dashed curve. In other words, adding the VT braces and strut fairings to the NASA-toboggan configuration results in a significant increase in noise reduction ranging from 0 to 1.84 dB for the array in position 1 and from 0.5 to 2.1 dB for the array in position 2.

On the flyover path, the lower truck components are not the only noise source components. The braces, lock-links, and the strut are also major landing gear noise components. Therefore, efficient landing gear noise reduction may be achieved if in addition to the truck, the braces and the strut are streamlined.

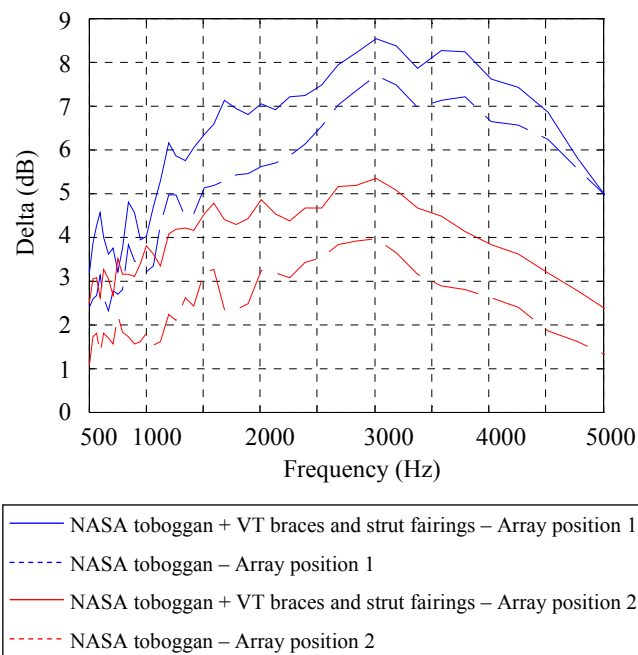


Figure 15: Noise reduction due to the NASA toboggan plus the VT braces and strut fairings (solid curves) and NASA toboggan alone (dashed curves) as estimated with the integrated spectra. The phased array was in the far-field in positions 1 (blue curves) and 2 (red curves).

Figure 16 shows the same results as Figure 14 except that the noise reduction was estimated from measurements conducted in the VT hard-walled wind tunnel, in the near-field of the model. On the flyover path, right under the gear, the landing gear noise reduction was estimated to be up to 15.2 dB at 2130 Hz. Noise reduction due to the VT-lower-truck fairing (red curve) is comparable to the one achieved by all the VT fairings combined (green curve). The NASA toboggan was shown to significantly reduce noise from the lower truck. In the near-field, noise generated by components behind the truck cannot be seen. Therefore, with the array in the near-field, the noise reduction achieved by the NASA toboggan on the overall landing gear noise is overestimated. For the same reasons, the VT-lower-truck fairing and all the VT fairings achieve comparable noise reductions.

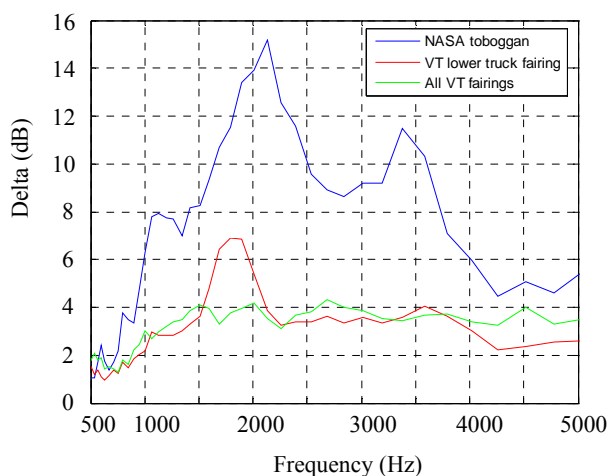


Figure 16: Noise reduction due to the NASA toboggan (blue curve), VT-lower-truck-fairing (red curve), and all VT fairings (truck, braces, and strut fairings - green curve) as estimated with the integrated spectra. Hard-walled test section - phased array in the near-field.

IV. Conclusion

The noise reduction potential of three fairings designed at Virginia Tech (VT fairings) and a fairing provided by NASA (NASA toboggan) was measured from far-field, streamwise, phased-array data collected in the VT aeroacoustic wind tunnel. With the phased array straight under the gear, results indicated that the NASA toboggan was the most efficient noise control device achieving up to 7.7 dB noise reduction at 3000 Hz. As the noise generated by the truck was reduced, other noise sources located behind the truck such as the leading edge of the door and the braces could be identified more clearly. On the rear arc, the effectiveness of the fairings was deteriorated. The NASA toboggan and the combination of all the VT fairings achieved comparable noise reduction. It was shown that for both far-field, phased-array positions, the VT braces fairing reduced significantly the noise radiated from the braces. Further noise reduction could be achieved by combining the NASA-toboggan and the VT braces and strut fairings. Through a comparison between measurements conducted in the semi-anechoic and hard-walled configurations of the VT wind tunnel, it was also shown that the noise reduction due to a fairing streamlining the truck will be largely overestimated if acoustic measurements are carried out in the near-field flyover path. The noise reduction due to fairings streamlining the landing gear components located behind the truck such as the braces and the strut will be misestimated since these components are not seen by the array in the near-field.

Acknowledgments

The authors would like to acknowledge the financial support from NASA Langley Research Center and its technical monitors Drs. Bart Singer and Mehdi Khorrami. The landing gear model used in this project was also provided by NASA. This financial support is greatly appreciated.

References

- ¹Davy, H., and Remy, R., "Airframe Noise Characteristics on a 1/11 Scale Airbus Model," *4th AIAA/CEAS Aeroacoustics Conference*, Toulouse, France, June 2-4, 1998. AIAA-1998-2335
- ²Dobrzynski, W., and Buchholz, H., "Full-Scale Noise Testing on Airbus Landing Gears in the German Dutch Wind Tunnel," *3rd AIAA/CEAS Aeroacoustics Conference*, Atlanta, GA, May 1997. AIAA-1997-1597-CP
- ³Dobrzynski, W., Chow, L. C., Guion, P., and Shiells, D., "Research into Landing Gear Airframe Noise Reduction," *8th AIAA/CEAS Aeroacoustics Conference*, Breckenridge, CO, June 17-19, 2002. AIAA 2002-2409
- ⁴Herkes, W. H., Olsen, R. F., and Uellenberg, S., "The Quiet Technology Demonstrator Program: Flight Validation of Airplane Noise-Reduction Concepts," *12th AIAA/CEAS Aeroacoustics Conference*, Cambridge, MA, May 8-10, 2006. AIAA 2006-2720
- ⁵Ravetta, P. A., Burdisso, R. A., Ng, W. F., Khorrami, M. R., and Stoker, R. W., "Screening of Potential Noise Control Devices at Virginia Tech for QTD II Flight Test," *13th AIAA/CEAS Aeroacoustics Conference*, Rome, Italy, May 21-23, 2007. AIAA 2007-3455
- ⁶Remillieux, M. C., Camargo, H. E., Burdisso, R. A., and W. F. Ng, "Aeroacoustic Study of a 26%-Scale, High-Fidelity, Boeing 777 Main Landing Gear in a Semi-Anechoic-Wind-Tunnel Test Section," *13th AIAA/CEAS Aeroacoustics Conference*, Rome, Italy, May 21-23, 2007. AIAA 2007-3453
- ⁷Ravetta, P. A., Burdisso, R. A., and W. F. Ng, "Noise Control of Landing Gears Using Elastic Membrane-Based Fairings," *13th AIAA/CEAS Aeroacoustics Conference*, Rome, Italy, May 21-23, 2007. AIAA-2007-3466
- ⁸Ravetta, P. A., "LORE Approach for Phased Array Measurements and Noise Control of Landing Gears," Ph.D. dissertation, Department of Mechanical Engineering, Virginia Polytechnic Institute and State University, 2005.
- ⁹Jaeger, S. M., Horne, W. C., and Allen, C. S., "Effect of Surface Treatment on Array Microphone Self-Noise," *6th AIAA/CEAS Aeroacoustics Conference*, Lahaina, HI, June 2000. AIAA-2000-1937
- ¹⁰Candel, S. M., "Application of Geometrical Techniques to Aeroacoustic Problems," *3rd Aeroacoustics Conference*, Palo Alto, CA, July 20-23, 1976. AIAA 1976-546
- ¹¹Pierce, A. D., *Acoustics, an Introduction to its Physical Principles and Applications*, Acoustical Society of America, Woodbury, NY, 1989.
- ¹²Remillieux, M. C., Camargo, H. E., and Burdisso, R. A., "Calibration of a Microphone Phased Array for Amplitude in the Virginia Tech Anechoic Wind Tunnel," *Noise Con*, Reno, NV, October 21-24, 2007.
- ¹³Soderman, P. T., and Allen, C. S., "Microphone Measurements In and Out of Airstream" in *Aeroacoustic Measurements*, Ed.T. J. Mueller, Springer Verlag, Berlin, 2002.